Preprints of the 19th World Congress
The International Federation of Automatic Control
Cape Town, South Africa. August 24-29, 2014

Adaptive Suppression of Inter-Area Oscillation using Multiple Wind Power Systems in a Distributed Parameter Control Methodology

Kaman S. Thapa Magar * **Mark J. Balas** ** **Dennice F. Gayme** ***

* *Department of Aersopace Engineering, Embry - Riddle Aeronautical University, Daytona Beach, FL, USA (e-mail: thapamak@erau.edu).*
** *Department of Aerospace Engineering, Embry - Riddle Aeronautical University(e-mail: balasm@erau.edu)*
*** *Mechnical Engineering Department, John Hopkins University(e-mail: dennice@jhu.edu)*

Abstract: This paper presents a preliminary study of using adaptive control of grid connected wind farms to damp the inter-area oscillations in wind integrated power systems. The power system is modeled as a distributed parameter systems using a forced first order hyperbolic wave equation, which represents an aggregate model for the system of coupled swing equations subject to wind farm power injections. A direct adaptive controller is used to stabilize the power swing in the face of disturbances using power injected from the wind farms at either a single or multiple locations throughout the power system.

Keywords: adaptive control, control of distributed systems, control of renewable energy resources, power system stability.

1. INTRODUCTION

The electricity generated from wind turbines is a growing proportion of the electrical power being injected onto existing transmission lines. The intermittent nature of power produced by wind turbines may have negative impact on the power grid. Therefore there has been a lot of work aimed at finding ways to mitigate these effect, see e.g. U.S. Dept. Energy (2008), Bousseau et al. (2006), Smith et al. (2007). Studies have also examined ways in which wind farms can be used to support the existing transmission system in adverse conditions. Some examples include using a wind farm to support the grid frequency (Aho et al. (2012)), controlling the wind turbine generator to stabilize the power systems after a disturbance (or grid fault)(Sakimoto et al. (2011)), and controlling power output of a wind farm to damp the inter-area oscillations (Chandra et al. (2013), Gayme and Chakrabortty (2013)).

Existing power systems are interconnected via transmission lines which carry bulk electrical power. Generators tend to be tightly coupled into areas in which the generators are synchronized (i.e. they all operate at the same frequency) (Kundur (1994)). The difference in this swinging of a group of generators in one area relative to those in an adjacent areas results in inter-area oscillations. These inter-area oscillations, if left undamped, can lead to grid stability issues that can have system wide consequences such as load shedding.

Flexible AC Transmission Systems (FACTS) are commonly used to damp inter-area oscillations as well as for other grid stability goals (Larson et al. (1995), Chaudhuri et al. (2003), and Majunmder et al. (2006)). Recent studies have examined the use of wind farm power output to stabilize the rotor swing (Miao et al. (2004), Gautam et al. (2009), and Tsourakis et al. (2010)) . Most of these techniques use the idea of controlling the Doubly Fed Induction Generators (DFIG) connected to the wind turbine to support the power system. Such control techniques do not consider the location of the wind power plant in new or existing power systems.

In paper by Gayme and Chakrabortty (2013) and Gayme and Chakrabortty (2012), it is shown that the location of a wind farm (i.e. the electrical distance along the transfer path at which the wind power is injected) greatly affects the spectrum of inter-area oscillation of the power systems. They further proposed the idea of controlling the wind farm power output to alter the spectrum of the power system to match a desired response (Gayme and Chakrabortty (2013)).

In this paper, the power system framework proposed by Gayme and Chakrabortty (2012) is used to study the effectiveness of an adaptive wind farm controller to damp the inter area oscillations due to disturbances in a large radial power system.

* This work was partially supported by the NSF Grant No. ECCS 1230788.

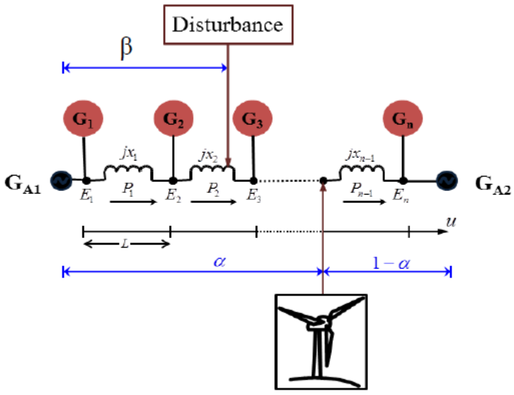

Fig. 1. A power system model with disturbance at β and wind farm power injection at α

2. POWER SYSTEM MODELING AND CONTROL

2.1 Power System as Distributed Parameter System

The power system under study is depicted in Fig. 1 where the generators in two different regions (G_{A1} and G_{A2}) are connected with a transmission line and series of generators. The generation G_i and power angle change δ_i of each generator are continuously distributed over the spatial dimension u. Assuming x_i andΔL to be the line reactance and spacing between generators G_i and G_{i+1} respectively, the rotor dynamics of the i^{th} generator can be expressed as (Cresp and Hauer (1981)):

$$\left(\frac{2H_i}{\Omega_i}\right) G_i\ddot{\delta}_i + \xi\dot{\delta}_i = P_i \quad \forall i = 1,2,......,n \tag{1}$$

where H_i is the inertia constant, $\Omega_s = 2\pi 60$ rad/sec is the electrical frequency with 60 Hz base, P_i is the net real power flowing out of i^{th} machine with $P_0 = 0$ and ξ is the damping coefficient. The real power flow from node i to $i+1$ over a lossless line is expressed as:

$$P_{i,i+1} = \frac{E_i E_{i+1} \sin(\delta_i - \delta_{i+1})}{x_i} \tag{2}$$

where E_i is the voltage magnitude at bus i. Assuming small changes in rotor angle and constant bus voltage of 1 per unit in equation (2), the net active power flow from the i^{th} machine can be approximated as:

$$P_i = P_{i-1,i} - P_{i,i+1}\frac{(\delta_{i-1} - \delta_i) - (\delta_i - \delta_{i+1})}{x_i} \tag{3}$$

Substituting (3) into (1) and dividing by ΔL we get:

$$\frac{2}{\Omega_i}\frac{H_i}{\Delta L}\ddot{\delta}_i + \frac{\xi}{\Delta L}\dot{\delta}_i = \frac{1}{\frac{x_i}{\Delta L}}\frac{(\delta_i - \delta_{i-1})}{(\Delta L)^2} - \frac{1}{\frac{x_i}{\Delta L}}\frac{(\delta_i - \delta_{i+1})}{(\Delta L)^2}.$$

Taking the limit as $\Delta L \to 0$ results in $\xi_{i-1} \to x_i$ and

$$\begin{aligned}&\frac{2}{\Omega_i}\frac{dH(u)}{du}\frac{dG(u)}{du}\ddot{\delta} + \frac{d\xi(u)}{du}\dot{\delta} \\ &= \lim_{\Delta x\to 0}\frac{1}{\frac{x_i}{\Delta L}}\frac{(\delta_{i+1} - 2\delta_i + \delta_{i-1})}{(\Delta L)^2} = \frac{1}{\frac{dx(u)}{du}}\delta_{uu}\end{aligned} \tag{4}$$

where $\frac{dG(u)}{du}$, $\frac{dH(u)}{du}$, $\frac{d\xi(u)}{du}$ and $\frac{dx(u)}{du}$ are respectively the generation, inertia, damping and reactance densities over the string of n generators. Considering an n link system each with an infinitesimal distance between each link $\Delta u_i \quad \forall i = 1,2,...n$; the average inertia density can be defined as:

$$H_T := \frac{1}{\sum_{i=1}^{n}\Delta u_i}\sum_{i=1}^{n}\frac{dH(u)}{du}\Delta u, \tag{5}$$

the average reactance density is:

$$\gamma := \frac{1}{\sum_{i=1}^{n}\Delta u_i}\sum_{i=1}^{n}\frac{dx(u)}{du}\Delta u, \tag{6}$$

and the average damping density is:

$$\eta := \frac{1}{\sum_{i=1}^{n}\Delta u_i}\sum_{i=1}^{n}\frac{d\xi(u)}{du}\Delta u, \tag{7}$$

The generation density is approximated by the total generation and is denoted by G_T. In the continuum as $n \to \infty$, the densities in (5)-(7) can be expressed as:

$$H_T = \frac{1}{L}\int_0^L dH(u) = \frac{H(L)}{L};\ \gamma = \frac{x(L)}{L};\ \eta = \frac{\xi(L)}{L}.$$

Substituting these expressions into (4) yields a damped hyperbolic wave equation in terms of the aggregated generator angle $\delta(u,t)$ as:

$$\frac{\partial^2\delta(u,t)}{\partial t^2} + \eta\frac{\partial\delta(u,t)}{\partial t} = \nu^2\frac{\partial^2\delta(u,t)}{\partial u^2} \tag{8}$$

with wave speed $\nu = \sqrt{\frac{377}{2H_T G_T \gamma}}$.

The corresponding power flow is:

$$P(u,t) = -\frac{1}{\gamma}\frac{\partial\delta(u,t)}{\partial u} \tag{9}$$

The system (8) represents an unforced system. Now adding a power injection (from an external source such as a wind farm) to (8) leads to:

$$\frac{\partial^2\delta(u,t)}{\partial t^2} + \eta\frac{\partial\delta(u,t)}{\partial t} - \nu^2\frac{\partial^2\delta(u,t)}{\partial u^2} = W(u,t) \tag{10}$$

where $W(u,t)$ is the net power injection. Assuming the power is injected at $u = \alpha$ as in Fig. 1, the net power injection can be expressed as:

$$W(u,t) = P_g(t)\hat{\delta}(u-\alpha) \tag{11}$$

where $\hat{\delta}(u-\alpha)$ is the Dirac delta function modeling a point source injection at a particular location in space and $P_g(t)$ is the net power injected.

2.2 Approximation of Hyperbolic PDE

To solve the hyperbolic PDE of (10), the power angle $\delta(u,t)$ and forcing function $W(u,t)$ are first expressed as the Fourier series:

$$\delta(u,t) = \frac{1}{2}A_0(t) + \sum_{n=1}^{\infty}[A_n(t)\cos(k_n u) + B_n(t)\sin(k_n u)] \tag{12a}$$

$$W(u,t) = \frac{1}{2}F_0(t) + \sum_{n=1}^{\infty}[F_n(t)\cos(k_n u) + G_n(t)\sin(k_n u)] \tag{12b}$$

where k_n are the wave numbers for each mode λ_n. Now, assuming G_{A1} and G_{A2} produce a constant power and no power is injected at both ends of the system, the power flow at the boundaries are constant in time. Then, the power angle $\delta(u,t)$ is a standing wave with zero slope at $u = 0$ and $u = 1$, which yields the boundary conditions:

$$P(0,t) = P(1,t) = 0. \tag{13}$$

Now, using these boundary conditions in (12a) and (12b) results in:

$$\delta(u,t) = \sum_{n=1}^{\infty} A_n(t)\cos(k_n u) = \sum_{n=1}^{\infty} A_n(t)\phi_n(u) \tag{14a}$$

$$W(u,t) = \sum_{n=1}^{\infty} F_n(t)\cos(k_n u) = \sum_{n=1}^{\infty} F_n(t)\phi_n(u) \tag{14b}$$

where $\phi_k(u) = cos(k_n u)$ are the spatial modes. Substituting (14a) and (14b) into (10) we get,

$$\frac{\partial^2 A_n(t)}{\partial t^2} + \eta\frac{\partial A_n(t)}{\partial t} + \nu^2 k_n^2 A_n(t) = F_n(t) \tag{15}$$

where $F_n(t)$ is obtained from the expression:

$$F_n(t) = 2\int_0^1 \cos(k_n u)\hat{\delta}(u-\alpha)du = 2P_g\cos(k_n\alpha). \tag{16}$$

2.3 Adaptive Control using Selective Modes

From (14a) it can be observed that the expression for power angle is a combination of spatial and temporal modes. The spatial modes are obtained using the boundary conditions whereas temporal modes are dictated by the expression in (15). In this paper, the boundary condition of (13) is considered which results in the approximate spatial modes of (Cresap et al. 1981):

$$\phi_k(u) = cos(k_n u) = cos\left(\frac{n\pi}{L}u\right) \tag{17}$$

Fig. 2 shows a plot of the first five spatial modes using a normalized distance between generation areas of $L = 1$.

From that the spatial injection location of a disturbance or wind power greatly affects the individual modes, e.g. injecting a power source at normalized distance of 0.15 encounters positive modal gain for the first three modes but negative modal gains for the fourth and fifth modes.

The temporal part of the aggregate rotor angle expression in (14a) is given by (15) which can be put in state-space form as:

$$\begin{bmatrix} \dot{A}_n(t) \\ \ddot{A}_n t \end{bmatrix} = \begin{bmatrix} 0 & 1 \\ -\nu^2 k_n^2 & -\eta \end{bmatrix}\begin{bmatrix} A_n(t) \\ \dot{A}_n(t) \end{bmatrix} + \begin{bmatrix} 0 \\ F_n(t) \end{bmatrix} \tag{18}$$

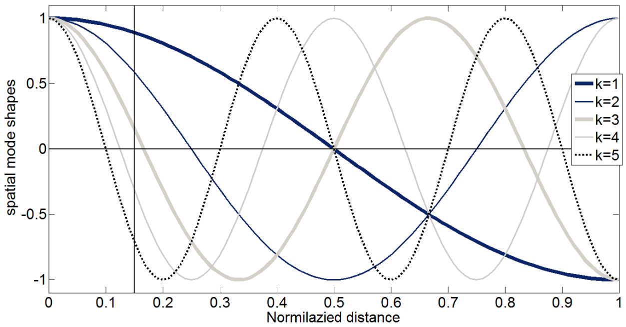

Fig. 2. First five spatial modes with normalized distance

Equation (18) is perturbed with $F_n(t)$ to get the temporal coefficient $\dot{A}_n(t)$ and this is combined with the spatial part of the PDE as in (14a) to get the power angle rate $\dot{\delta}(u,t)$ as:

$$\dot{\delta}(u,t) = \sum_{n=1}^{\infty} \dot{A}_n(t)\cos(k_n u) = \sum_{n=1}^{\infty} \dot{A}_n(t)\phi_n(u) \tag{19}$$

$\dot{\delta}(u,t)$ in (19) is measured at a specified location in the power system. But for simulation, it is not possible to take an infinite number of modes, hence the summation is truncated at some specified number of modes N, which results in:

$$y := \dot{\delta}_{est}(u,t) = \sum_{n=1}^{N} \dot{A}_n(t)\cos(k_n u) = \sum_{n=1}^{N} \dot{A}_n(t)\phi_n(u) \tag{20}$$

In simulation the approximated rotor angle rate $\dot{\delta}_{est}(u,t)$ is used as output.

A large power system is very complex system and hence modeling errors are unavoidable. Also, the presence of different kinds of generator sources and loads make it difficult to assess the power system parameters. An adaptive controller is best suited in such conditions because of its capability to adapt the gains and perform under these types of errors and uncertainties.

Now based on the system configurations (14a), (16), (18), (19), and (20), we select an adaptive controller (Magar et al. (2012)) to damp the rotor angle swing. The proposed controller takes the rotor angle rate at specified spatial point as input and produces the torque command to the wind farm:

$$\begin{aligned} T_g(t) &= G_e\dot{\delta} + G_D\phi_D \approx G_e\dot{\delta}_{est} + G_D\phi_D \\ &= G_e y + G_D\phi_D \end{aligned} \tag{21}$$

where G_e and G_D are the adaptive gains based on the gain adaption laws:

$$\dot{G}_e = -\dot{\delta}^2\gamma_e \approx -\dot{\delta}_{est}^2\gamma_e = -y^2\gamma_e$$
$$\dot{G}_D = -\dot{\delta}\phi_D\gamma_D = -y\phi_D\gamma_D.$$

In these expressions γ_e and γ_D are the positive definite gain matrices.ϕ_D is the basis function for the disturbance, which is assumed to be generated from disturbance model of the form:

$$\begin{cases} u_D = \Theta z_D;\ z_D = L_D \phi_D \\ \dot{z}_D = F z_D; z_D(0) = z_0 \end{cases} \tag{22}$$

where Θ, L_D, and F are the matrices that determine the known form of disturbance waveforms. In the adaptive control law (21), the first tem is responsible for driving the measured output (i.e. rotor angle rate $\dot{\delta}$) to zero whereas the second term is responsible for driving disturbances to zero.

In order to guarantee stability and convergence of the adaptive controller (20) with gain adaption laws (21), the system under study has to be Almost Strict Positive Real (ASPR), i.e. the plant transfer function has to be minimum phase and the high frequency gains (product CB) has to be positive (Balas and Fuentes (2004)) where C and B are the output and input gain matrices for the state space description (A, B, C) of the combined system (18) - (20).

3. ADDITION OF WIND FARM DYNAMICS

An adaptive control strategy based on selected modes of the power system is proposed in the previous section. In this section wind farms are used with the adaptive controller to damp the inter-area oscillation modes.

A third order aggregate wind farm model developed in Sloth et al. (2010) is used to study the effectiveness of adaptive controller to damp the oscillation due to disturbance in the power system. A linearizion proposed wind farm discussed in Gayme and Chakrabortty (2013) has the transfer function of the form:

$$G_w(s) = \frac{P_g(s)}{T_g(s)} = \frac{6.786s + 1.939e4}{s^3 + 0.294s^2 + 816.2s + 0.7696} \tag{23}$$

where $P_g(s)$ is the Laplace transform of the wind farm power output and $T_g(s)$ is the Laplace transform of torque input for each wind farm.

Since the basic idea behind damping the inter-area oscillation is to control the power output of the wind farm using an adaptive controller under disturbances to the power system, the wind farm in (24) can be viewed as actuator dynamics connecting the power system and the adaptive controller.

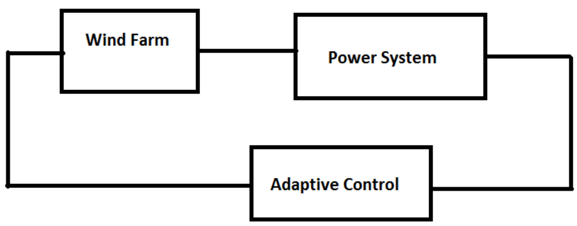

Fig. 3. Schematics of using adaptive controller with wind farm

A schematic for adding the wind farm to the power system is in Fig 3. The power system block corresponds to the model developed in (18), (19), the wind farm block corresponds to the wind farm model of (23) and the adaptive control block corresponds to the controller proposed in (21), (22). From (18) and (19) we can observe that the transfer function for the temporal response of each mode of power system has form:

$$P_{sys}(s) = \frac{s}{s^2 + \eta s + \nu^2 k_n^2} \tag{24}$$

This transfer function has the relative degree of one. When the power system is constructed using multiple modes, then the corresponding transfer functions based on (24) with different parameters are connected in parallel. The transfer function obtained from the parallel combination of (24) also retains the relative degree of one. Hence, the power system block will have a transfer function of relative degree one. Also from (23), the wind farm transfer function has relative degree of two. Since the wind farm acts as an actuator for the power system which is actuated with the signal obtained from the adaptive controller, the combination of the wind farm and the power system can be assumed as a single block for adaptive controller implementation. When the wind farm and the power system are combined in series, the combined block will now have relative degree of three. This transfer function when converted to state space form will produce the product $CB = 0$; or the high frequency gain will be zero. Since the proposed adaptive controller requires the product $CB > 0$ for stability, a feedforward path is needed in the wind farm to change its relative degree to zero which results in the combination of wind farm and power system to have a relative degree of one.

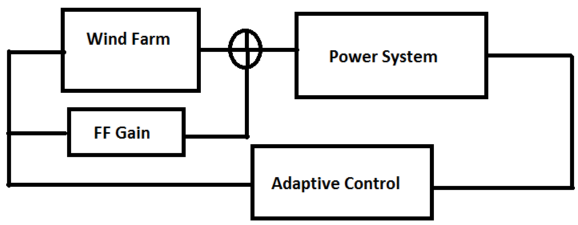

Fig. 4. Using FF path in wind farm to comply with ASPR requirement

A feedfoward path with a gain of 90 is used as shown in Fig. 4 to make the overall system ASPR (i.e. such that the product $CB > 0$ and the system is minimum phase).

4. SIMULATION

For the study of the effectiveness of the adaptive controller in damping the rotor angle swing, the system is setup according to the description in previous sections. The parameters for the power system and wind farm were used from Sloth et al (2010). Only the first five modes are used to illustrate the theory presented in the previous sections.

A step disturbance of magnitude 0.25 p.u. is injected at distance of 0.5 along the electrical transfer path and two identical wind farms are assumed to be installed at respective distances of 0.12 and 0..75. Adaptive controllers are used to control power output of these two wind farms

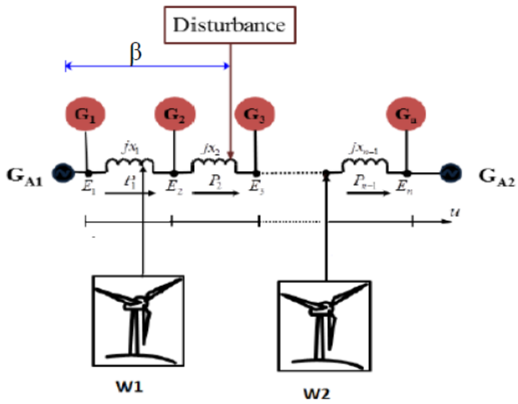

Fig. 5. Schematics of using two wind farms to damp inter area oscillation

based on the rotor angle rate measurement of (20) at these places.

The schematic for using two wind farms to damp the inter-area oscillation is shown in Fig. 5. The rotor angles are observed at different locations considering each individual wind farm and the combination of both wind farms.

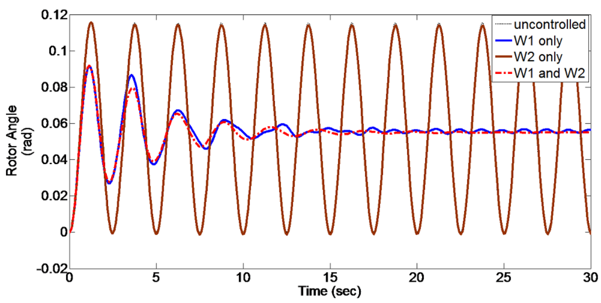

Fig. 6. Rotor angle profile at 0.12 under different conditions

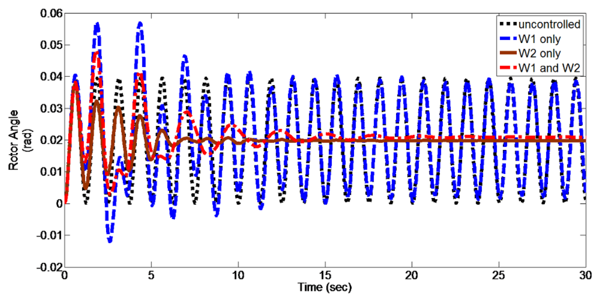

Fig. 7. Rotor angle profile at 0.75 in different conditions

The rotor angle profiles at distance of 0.12, 0.5 and 0.75 are plotted in Fig 6, Fig. 6, and Fig. 8 respectively. Each figure shows the rotor angle profile for different controlled conditions e.g. uncontrolled, controlled with W1, controlled with W2 and controlled with both W1 and W2.

From the figures it can be seen that the controller has good local performance when using only one wind farm but the combination of two wind farms results in better performance throughout the system. In another words, using two wind farms are more effective in damping the inter - area oscillations throughout the full range of interest compared to using only one wind farm.

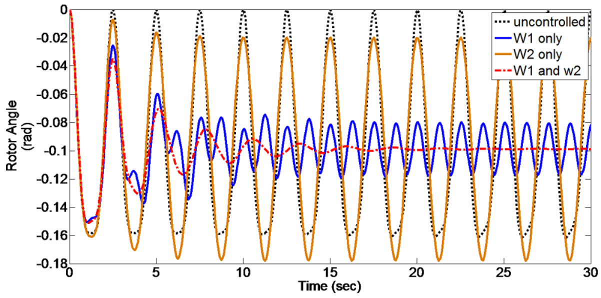

Fig. 8. Rotor angle profile at 0.5 in different conditions

5. CONCLUSIONS

Use of an adaptive controller to damp the inter-area oscillations is discussed in this paper. The power system is modelled as a distributed parameter system using a forced second order hyperbolic PDE. The first five modes of the system were considered for the simulation. A third order wind farm model along with an adaptive controller is used at two different locations to stabilize the rotor angle swing in the face of the power system disturbances. From the rotor angle profile at three different locations, it is found that co-ordinated control of multiple wind farms effectively damps the rotor swing throughout the system whereas the single wind farm is only effective in locally damping the rotor swing.

REFERENCES

Aho, J., Buckspan, A., Lacks, J., Fleming, P., Yunho, J., Dune, F., Churchfield, M., Pao, L., and Johnson, K. (2012). A tutorial of wind turbine control for supporting grid frequency through active power control. In *Proceedings of American Control Conference (ACC)*, 3120–3131.

Balas, M. and Fuentes, R. (2004). A non-orthogonal projection approach to characterization of almost positive real systems with an application to adaptive control. In *Proceedings of American Control Conference (ACC)*.

Bousseau, P., Fesquet, F., Belhomme, R., Nguefeu, S., and Thai, T.C. (2006). Solutions for the grid integration of wind farm - a survey. *Wind Energy*, 9.

Chandra, S., Gayme, D.F., and Chakrabotty, A. (2013). Coordinating wind farms and battery management systems for inter-area oscillation damping: A frequency-domain approach. *IEEE Trans. on Power Systems*, PP, 1–9.

Chaudhuri, B., Pal, B., Zolotas, A.C., Jaimoukha, I.M., and Green, T.C. (2003). Mixed-sensitivity approach to h-∞ control of power system oscillations employing multiple facts devices. *IEEE Trans. on Power Systems*, 18, 1149 – 1156.

Cresp, R.L. and Hauer, J.F. (1981). Emergence of a new swing mode in the western power loop. *IEEE Trans. on Power Apparatus and Sys.*, PAS-100, 2037–2045.

Gautam, D., Vittal, V., and Harbour, T. (2009). Impact of increased penetrations of dfig based wind turbine generators on transient and small signal stability. *IEEE Trans. Power Syst.*, 24, 1426 –1434.

Gayme, D.F. and Chakrabortty, A. (2012). Impact of wind farm placement on inter-area oscillations in large power systems. In *Proceedings of American Control Conference (ACC)*.

Gayme, D.F. and Chakrabortty, A. (2013). A spatio-temporal framework for spectral analysis and control of inter-area oscillations in wind-integrated power systems. *IEEE Trans. on Control Systems Technology*, PP, 1 – 8.

Kundur, P. (1994). *Power System Stability and Control*. McGraw - Hill Education, New York City, NW.

Larson, E.V., Sanchez-Gesca, J.J., and Chow, J.H. (1995). Concepts for design of facts controllers to damp power swings. *IEEE Trans. Power Syst.*, 10, 948 –956.

Magar, K.T., Balas, M., and Frost, S.A. (2012). Adaptive disturbance tracking control with wind speed reduced order state estimation for region ii control of wind turbine. In *Proceedings of ASME 2012 Conference on Smart Materials, Adaptive Structures and Intelligent Systems (SMASIS 2012)*.

Majunmder, R., Pal, B.C., Dutfour, C., and Korba, P. (2006). Design and real-time implementation of robust facts controller for damping inter-area oscillation. *IEEE Trans. Power Syst.*, 21, 809 –816.

Miao, Z., Fan, L., Osborn, D., and Yuvarajan, S. (2004). Control of dfig based wind generation to improve inter-area oscillation damping. In *Proc. IEEE Power & Energy Soc. GM'09*.

Sakimoto, K., Miura, Y., and Ise, T. (2011). Stabilization of a power system with a distributed generator by a virtual synchronous generator function. In *Proceedings of Power Electronics and ECCE Asia (ICPE & ECCE), 2011 IEEE 8th International Conference on*.

Sloth, C., Esbensen, T., and Stoustrup, J. (2010). Active and passive fault-tolerant lpv control of wind turbines. In *Proceedings of American Control Conference (ACC)*.

Smith, J.C., Milligan, M.R., DeMeo, E.A., and Parsons, B. (2007). Utility wind integration and operating impact state of art. *IEEE Trans. on Power Systems*, 22, 900 – 908.

Tsourakis, G., Nomikos, B.M., and Vournas, C.D. (2010). Contribution of doubly fed wind generators to oscillation damping. *IEEE Trans. Energy Convers.*, 24, 783 –791.

U.S. Dept. Energy (2008). 20 % wind energy by 2030: Increasing wind emergy's contribution to u.s. electricity supply. Technical Report DOE-GO - 102008-2567, U.S. Dept. Energy, Nat. REnew. Energy Lab, Golden, CO, USA.